An inter-comparison of regional climate models for Europe:

Model performance in Present-Day Climate

Daniela Jacob[1], Lars Bärring[5], Ole Bøssing Christensen[2], Jens Hesselbjerg Christensen[2], Manuel de Castro[11], Michel Déqué[8], Filippo Giorgi[10], Stefan Hagemann[1], Martin Hirschi[3], Richard Jones[9], Erik Kjellström[5], Geert Lenderink[6], Burkhardt Rockel[7], Enrique Sánchez[11],Christoph Schär[3], Sonia I. Seneviratne[4*], Samuel Somot[8], Aad van Ulden[6], Bart van den Hurk[6]

[1]Max Planck Institute for Meteorology, Bundesstr.53, 20146 Hamburg, Germany

[2]Danish Meteorological Institute, Lyngbyvej 100, 2100 Copenhagen, Denmark

[3]Institut for Atmospheric and Climate Science ETH, 8057 Zürich, Switzerland

[4]Global Modeling and Assimilation Office NASA, Goddard Space Flight Center, Greenbelt, USA

[5]Rossby Centre, SMHI, 60176 Norrköping, Sweden

[6]Royal Netherlands Meteorological Institute, 3730 AE de Bilt, The Netherlands

[7]GKSS Forschungszentrum Geesthacht, Max-Planck-Strasse, 21502 Geesthacht, Germany

[8]Météo-France CNRM, 42 av. Gaspard Coriolis / 31057 Toulouse Cedex / France

[9]Met Office Hadley Centre (Reading Unit), Meteorology Building, University of Reading, RG6 6BB, United Kingdom

[10]The Abdus Salam International Centre for Theoretical Physics, P.O. BOX 586, 34100 Trieste, Italy

[11]Facultad de Ciencias del Medio Ambiente, Universidad de Castilla-La Mancha, Avda. Carlos III, s/n 45071 Toledo, Spain

* present affiliation: Institute for Atmospheric and Climate Science ETH, Zürich, Switzerland

submitted to:

Climatic Change, Special Issue: PRUDENCE

corresponding author:

Daniela Jacob, Max-Planck-Institute for Meteorology, Hamburg, Germany

Jacob@dkrz.de

Abstract

The analysis of possible regional climate changes over Europe as simulated by ten regional climate models within the context of PRUDENCE requires a careful investigation of possible systematic biases in the models. The purpose of this paper is to identify how the main model systematic biases vary across the different models.

Two fundamental aspects of model validation are addressed here: the ability to simulate i) the long-term (30 or 40 years) mean climate and ii) the inter-annual variability. The analysis concentrates on near-surface air temperature and precipitation over land and focuses mainly on winter and summer. In general, there is a warm bias with respect to the CRU data set in these extreme seasons and a tendency to cold biases in the transition seasons. In winter the typical spread (standard deviation) between the models is 1K. During summer there is generally a better agreement between observed and simulated values of inter-annual variability although there is a relatively clear signal that the modeled temperature variability is larger than suggested by observations, while precipitation variability is closer to observations. The areas with warm (cold) bias in winter generally exhibit wet (dry) biases, whereas the relationship is the reverse during summer (though much less clear, coupling warm (cold) biases with dry (wet) ones). When comparing the RCMs with their driving GCM, they generally reproduce the large-scale circulation of the GCM though in some cases there are substantial differences between regional biases in surface temperature and precipitation.

1. Introduction

Increasing greenhouse gas (GHG) concentrations, changing aerosol composition and load as well as land surface changes are influencing the climate of the Earth, globally as well as regionally. Global climate models are investigating possible trends in future global climate through the development of climate change scenarios. These follow specific assumptions for the evolution of greenhouse gases and aerosols, several of which have been defined by the Intergovernmental Panel on Climate Change (IPCC, Houghton et al., 2001) and are described in the IPCC Special Report on Emission Scenarios (SRES, Nakicenovic et al, 2000). Unfortunately, due to the lack of computer power, global climate models are generally still not able to represent surface heterogeneities on scales less than about 100 km. However, global climate change has an influence on these local and regional scales which will be experienced by human kind directly.

Improved information on regional climate change can be achieved with the use of different regionalization techniques, including high-resolution and variable resolution AGCMs (Cubasch et al. 1995, Déqué and Piedelievre 1995), nested regional climate models, or RCMs (Giorgi and Mearns 1999), and statistical downscaling (Wilby et al. 1998).

In the present study, the performance of 9 different RCMs and one variable resolution AGCM in reproducing present-day climate over the European region is investigated. These models were used as part of the European project PRUDENCE (Christensen et al. 2002) to produce climate-change simulations over the European region and to analyze the uncertainty associated with these simulations.

Two sets of 30-year simulations were completed by all models, one for the present day period of 1961-1990 and one for the future time period of 2071-2100 under forcing from the A2 IPCC scenario.

This paper focuses on the validation of the 1961-1990 present-day simulations as input to the assessment of the models' response to climate change. Other papers presented in the special issue focus on the climate change scenarios. The primary aim of this paper is to identify how the main model systematic biases vary across the different models. We emphasize that, by experimental design, the models use comparable resolution and domain as well as the same forcing lateral boundary conditions. Thus the influence of factors specific to the internal model physics and dynamics can be determined. This experiment design also allows the identification of features that are common or vary across the ensemble of models.

The performance of the models has been evaluated through an agreed validation strategy, which has been worked out by the participating groups. It includes the comparison of simulated seasonal and annual means against observations as well as a comparison of observed and simulated inter-annual variability for temperature. These results determine the level of confidence for the driving models as well as for the regional-scale details.

A description of the experimental design is given in section 2, while the analysis of model performances for today's climate is presented in section 3 and the conclusions are presented in section 4**.**

2. Design of the experiment

The overall idea behind PRUDENCE was to establish a large ensemble of regional climate-change simulations for Europe for the time frame of 2070 to 2100 (Christensen et al, this issue). The overall focus on assessing sources of uncertainty of the project made a careful design of the ensemble to sample uncertainties in an efficient manner intractable, but the present set-up represents an ensemble of possibilities.

2.1 Description of the models

A short description of the participating RCMs is given in Table 2.1 together with information about the global atmospheric climate model HadAM3H (Buonomo et al., 2006), which was chosen to be the central GCM delivering lateral boundary conditions to the RCMs used for the PRUDENCE Standard Ensemble. In the following the names of the models as they are used within this paper are introduced in alphabetical order together with the main references.

The PRUDENCE Standard ensemble:

ARPEGE (Gibelin and Déqué 2003), **CHRM** (Vidale et al, 2003), **CLM** (Steppeler et al., 2003), **HadRM3H** (Buonomo et al., 2005), **HIRHAM** (Christensen et al., 1996), **RACMO** (Lenderink et al., 2003), **RCAO** (Döscher et al., 2002, Jones et al., 2004, Meier et al., 2003), **RegCM** (Giorgi and Mearns 1999), **REMO** (Jacob, 2001) and **PROMES** (Castro et al., 1993).

2.2 Description of the simulations

Christensen and Christensen (in this issue) describe the overall experiment set-up that was utilized within PRUDENCE. Here only a very brief description of the simulations used within this study is given. For further details see Christensen and Christensen.

The experiments cover a time period from 1961 to 1990. All RCM simulations have been carried out over Europe using 6 hourly lateral boundary conditions provided by HadAM3H along with sea surface temperature (SST) and sea ice conditions estimated from observations for current climate, i.e. the HadISST dataset (Rayner et al., 2003). ARPEGE requires only surface boundary conditions (i.e. sea ice and SST) which are also taken from the HadISST dataset. In terms of SSTs and sea ice conditions RCAO is an exception in that it calculates those properties explicitly in the Baltic Sea and Kattegat (Döscher et al., 2002; Räisänen et al., 2004).

The RCMs used their own model setup as well as grid specification like rotation and number of vertical levels but similar horizontal resolutions of about 50 km (Table 2.1). Some analyses presented in this paper also include information from simulations with HIRHAM carried out at 25 and 12km resolution and a 25km version of RCAO, as indicated in the related sections. The HIRHAM high-resolution experiments have been driven by the same lateral and lower boundaries as the 50km simulations, except that the 12-km simulation uses the Baltic SSTs from the RCAO 50km simulation as does the high-resolution RCAO.

3. Model performance

3.1 Systematic errors and inter-annual variability

Two fundamental aspects of model validation are addressed here: the ability to simulate i) the long-term (30 or 40 years) mean climate and with less detail ii) the inter-annual variability. The analysis concentrates on near-surface air temperature and precipitation over land and focuses mainly on the winter and summer seasons (December-January-February (DJF), June-July-August (JJA)), though the transition seasons of March-April-May (MAM) and September-October-November (SON) are also considered. For a nested model, it is well known that the ability to simulate these quantities depends to a large degree on the quality of the driving model, and in particular on the degree to which the driving model represents the observed flow conditions for the region of concern (*e.g.* Noguer et al., 1998, Machenhauer et al., 1998; Christensen et al. 1998; Giorgi et al. 2001). Therefore, first the systematic mean flow errors in the baseline PRUDENCE driving model HadAM3H are investigated.

In order to analyze the models' ability to simulate near-surface air temperature and precipitation, 8 sub-regions are used (*e.g.* Figure 4 in Christensen and Christensen, this issue). Note that only land points have been used in all investigations. A comparison of the simulated 30-year mean climatology with the one of the 0.5° by 0.5° gridded climatology provided by the Climate Research Unit (CRU) of the University of East Anglia (Hulme et al., 1995) is carried out, as well as a study of the inter-annual variability thereof (New et al., 2000, 2002).

3.1.1 HadAM3H Mean Sea Level Pressure Bias

The currently best available climatology documenting the present seasonal mean atmospheric flow conditions are provided by the reanalysis projects at NCEP (Kalnay et al, 1996) and ECMWF (ERA15: Gibson et al., 1997, ERA40: Simmons and Gibson, 2000). For Europe, the ERA15 and ERA40 re-analyses only differ slightly, and therefore only the ERA40-reanalyses of ECMWF is used here. Figure 3.1.1 compares the 40-year climatology of mean sea level pressure (MSLP) for DJF and JJA from ERA40 with the 30-year climatology of the PRUDENCE baseline experiment using HadAM3H. Machenhauer et al. (1998) concluded that the difference between a 20- and 30-year climatology appeared to be much less of an issue than the difference between observed and modeled conditions. This is confirmed by comparing the ERA40 climatology with the older ERA15 climatology (not shown).

The main winter-time features to observe from Figure 3.1.1 are that HadAM3H provides a reasonably good simulation of the mean sea level pressure pattern though it exhibits a stronger pressure gradient across a large part of central to northern Europe than the reanalysis. This is caused by too high pressure over the Mediterranean region and too deep Icelandic low extending too far into the Nordic seas. As a consequence, the moisture and heat transport (in the mean as well as from eddies) from the Atlantic sector to most of Northern Europe is too high, leading in general to excessively high temperatures and precipitation rates. Van Ulden et al. (2005) estimated the contribution of the enhanced westerly circulation to the temperature in central Europe to be 0.8 ^{o}C, and 0.4 mm day^{-1} for precipitation (which are generally smaller than typical model errors, Figure 3.1.3). It is less certain what this means for Southern Europe as this also depends on the balance between energy and moisture transport in the mean field and from the eddies (see *e.g.* Machenhauer et al. 1998). Note that ARPEGE (the only model not forced at the lateral boundaries by HadAM3H) has the same kind of MSLP bias as HadAM3H in winter (see Gibelin and Déqué, 2003). The

consequence is the same: too high temperature and precipitation rates over Northern Europe and too low temperature and precipitation rates over Southern Europe.

In summer HadAM3H is closer to ERA40. However, it is noticed that the MSLP in HadAM3H is more homogeneous over most of the continent and has a less pronounced Azorean high. Therefore westerly flow into this region is reduced and the region with subsiding air over Europe is displaced somewhat to the east. These would imply less moisture transport to this region than suggested by observations, leading to too dry and warm conditions (see also Machenhauer et al. 1998 and related work in PRUDENCE). This behavior is less important in ARPEGE, where the Eastern warm bias is reduced.

3.1.2 RCM Mean Sea Level Pressure Deviations to the Driving GCM

Winter RCM average results, as they are basically controlled by large-scale processes, are very close to GCM results (fig.3.1.2a, ARPEGE not included). Nevertheless, some patterns, such as Iberian Peninsula pressure or Balkans high pressures, seem to be better defined in the RCM ensemble mean. High pressure values over southern Europe are slightly higher than GCM ones. For the summer season, differences between GCM and RCM mean fields are more important. This can be explained by a weaker atmospheric circulation and the increasing relevance of smaller scale processes for this season compared with winter behavior. Values and pressure structure for southern, western and Central Europe are closer to ERA40 values than GCM results. For example, relative low pressures over the Iberian peninsula are higher than GCM values, and are closer to ERA40 results. The same is evident over France and most of Central Europe.

Figure 3.1.2b summarizes the mean sea level deviations in the RCMs for DJF and JJA, respectively. The figure compares the ensemble mean deviation from the driving HadAM3H MSLP field for the area of maximum model overlap (two models do not go further north and one model does not cover the Mediterranean region). The inter-model standard deviation is also shown by black contours. The largest values occur over mountainous regions. The model mean deviation from the driving model is always small, with the largest differences over mountainous regions. The latter can partly be explained by different algorithms for computing the diagnostic mean sea level pressure from the mean surface pressure in the various models and in the driving model and by different horizontal resolutions. This is also reflected by the relatively high inter-model standard deviation in these regions. During summer, there is a tendency towards a general increase of pressure in the eastern part of the region of subsidence (East-Europe), which would indicate that the RCMs could be enhancing the expected dry and warm bias imposed by the boundary conditions as indicated above. However, as we shall see in the following sections, this model behavior is not true in all cases (see also van Ulden *et al.* 2005 – this volume)

3.1.3 Near surface air temperature and precipitation

Figure 3.1.3 is an illustration of the sign and magnitude of model biases for the 8 sub-standard regions (from Christensen and Christensen, this issue). The left column shows temperature bias in degrees for the 4 seasons, and the right column shows relative bias of precipitation in absolute numbers. Red indicates a positive bias and blue a negative; white is zero, and the black squares are out-of-range flags for the regions not covered by the particular model. All resolutions and models are compared to the CRU data. HadAM3H is the driving model, and "Ensemble" indicates the average of the ten 50km RCM experiments (the nine RCMs of the PRUDENCE standard ensemble plus an additional

HIRHAM version run at the Norwegian Met Office) covering the region in question and the stretched global model ARPEGE.

Tables 3.1.3a and b summarize the winter and summer seasonal mean model temperature bias with respect to the CRU climatology for each of the 8 regions as well as the inter-annual standard deviation. The tables also include information from simulations with HIRHAM carried out at 25 and 12km resolution, a 22km version of the RCAO model, results from the driving GCM (HadAM3H). Also shown is the 11-member ensemble mean based only on the 50km model versions.

Generally, horizontal patterns in Fig. 3.1.3. indicate that the model bias is largely induced by the lateral boundary forcing (e.g. precipitation in DJF), while the vertical ones show that the bias originates to a large extent from within the model domains (*e.g.* temperature in MAM). There is however no clear tendency towards a common pattern in both temperature and precipitation, except for DJF, when both temperature and precipitation seem to be dominated by large scale forcing. The areas with warm (cold) bias in winter generally exhibit wet (dry) biases, whereas the relationship is the reverse during summer (though much less clear, coupling warm (cold) biases with dry (wet) ones). Even ARPEGE, which is not forced at the lateral boundaries by HadAM3H, shows the same behavior as the other RCMs in winter. The too zonal winter climate of the HadAM3H and ARPEGE simulations is reflected in the wet climate in central and northern Europe in contrast to the dry climate in the Mediterranean region. For MAM it is not possible to detect clearly if the temperature and precipitation biases are internally generated or imposed by the boundaries, and a similar pattern may be noticed in SON. In JJA no clear picture emerges, except for eastern Europe (EA), where the warm and dry bias clearly follows the tendency of the driving HadAM3H. ARPEGE and PROMES are the

only two models for which the JJA temperature bias is less than 1 K over the EA region whereas the driving model and the RCM ensemble mean show a bias close to 2 K over this region.

Regarding temperature it should be noted that a constant vertical lapse rate of 6.5 K/km has been used to refer all grid points to a common altitudes. This constant lapse rate introduces an uncertainty in the temperature comparisons, especially in mountainous regions. In general, there is a warm bias with respect to the CRU data in the extreme seasons and a tendency to cold biases in the transition seasons.

In winter this warm bias is particularly strong over Scandinavia (SC; more than 2K) except for ARPEGE (bias less than 0.2 K); as an exception the southernmost region MD (Mediterranean) tends to be too cold (bias around -0.5K) and dry (bias around -1 mm/day). A typical spread (standard deviation) between the models is 1K. This warm bias is consistent with the systematic bias in the MSLP as explained above. It could also be influenced by a possible cold bias in the CRU data set in Scandinavia (Christensen at al., 1998). high inter-annual variability in the observations makes this difference less significant (the CRU mean temperature is only claimed to be accurate to within approximately 1K). The inter-annual variability of the regional models is reduced compared to observations in most areas in winter, particularly in northern and western Europe (Table 3.1.3a – right columns). Van Ulden et al. (2005) showed that in winter the driving HadAM3H is too zonal and simulates insufficient blocking frequencies, which are the main source for the inter-annual variability in this season.

In summer, CLM and especially PROMES are too cold, whereas most of the other models are too warm and dry with HadRM3H and the high resolution simulation with RCAO show the most extreme behavior and ARPEGE shows the smallest bias. For JJA, the ensemble mean model bias is in general

lower than in winter (with the exceptions of MD and EA). This is consistent with the bias in the MSLP as explained above (see also Noguer et al., 1998, Machenhauer et al. 1998). During summer there is generally a better agreement between observed and simulated values of inter-annual variability although there is a relatively clear signal in that most of the modeled temperature variability is larger than suggested by observations, while precipitation variability is closer to observations (cf. Table 3.1.3b). This finding is not easy to interpret. However, the different formulations of the model surface schemes, particularly during this season, offer one possible source for this variability. The causes of the overestimation of the summer temperature variability are further analyzed by Lenderink et al. (2005). The well-known summer drying of many RCMs is reflected in the blue colors for areas MD and especially EA in JJA; the strength of the dry bias varies (Tab. 3.1.4b), however. RegCM has too high precipitation, HIRHAM and RACMO are close to the mean, ARPEGE and REMO have a very modest bias, whereas RCAO, PROMES and CHRM are quite dry. Note that EA in reality is very dry during summer, but the exaggerated lack of rain dries out soil water reservoirs in many models causing very high surface temperatures in late summer.

The inter-annual variability of precipitation is in relative good agreement with observations for both winter and summer. The most anomalous model with respect to precipitation is the CHRM model which is consistently much drier than the others. However, it is on the cold side during summer. These drying problems are enhanced by a circulation bias of HadAM3H, which simulates too frequent blocking events in summer, accompanied by dry and sunny circulations from the east (Van Ulden et al., 2005).

3.1.4 RCM temperature and precipitation deviations from the driving GCM

From figure 3.1.3 it is also clear in many regions, RCM biases differ from those in the GCM. In some cases, there is even a general model tendency independent of region, e.g. RCAO and REMO are generally warmer than HadAM3H in all seasons with CHRM drier and CLM wetter. This indicates that though the main circulation features are being reproduced by the RCMs, their different configurations are leading to simulations which deviate from the GCM performance over large regional scales.

3.*1.5 Resolution issues and the ensemble mean model.*

A comparison of the HIRHAM experiments at different resolution as well as between the two RCAO experiments shows that change of resolution has a minor impact on large-scale climate features. There is a small increase in precipitation with resolution.

By a simple ranking procedure area by area and season by season it can be determined that the ensemble mean performs better than individual models: It is the best "model" with respect to temperature and MSLP and number four with respect to precipitation among the 50km RCMs. Furthermore the mean model is less prone to having large deviations in particular areas; it tends to have similar quality for most areas.

In winter, as seen in Fig. 3.1.3, the ensemble mean exhibits the same warm and wet bias as most individual models. This again reflects the fact that the winter climate in the regional models is strongly forced by the boundary conditions. In summer the mean model performs very well, with the exception of Eastern Europe and to a lesser degree the Mediterranean, where the aforementioned warm and dry bias prevails.

The bias of the ensemble mean is generally below 1K and in only one case above 2K. This is Scandinavia in winter, where the CRU data might also be uncertain (see above). The precipitation bias is generally below 0.5 mm/day and never more than 1 mm/day. In relative terms most values are less than 30% in error and always less than 50%.

3.2 Ranges of minimum and maximum temperatures

The ability of the RCMs to simulate daily variability of T2m, T2min and T2max is investigated in Kjellström et al. (2005). They compare simulated control to observations from the European Climate Assessment (ECA) dataset (Klein Tank et al., 2002a, 2002b). Here, we summarize some of their findings focussing on extremely warm summer and extremely cold winter conditions.

Empirical distributions of the temperature variables are calculated from the RCMs and from the ECA observations. Biases for different percentiles from these distributions are compared for summer (JJA) and winter (DJF) in different European regions. Table 3.2, which shows the median bias among the RCMs in different regions, indicates that the positive bias in most of Europe (BI, IP, F, ME, SC and MD) in winter is larger at the 1st and 5th percentiles than in the median. This is a broad-scale feature among the models seen in large parts of the probability distributions both for T2m and T2min.

In summer, the strong bias seen in monthly mean T2max and T2m in east Europe (EA) is more pronounced in the 99th and 95th percentiles in both variables. The cold bias in Scandinavia (SC) during summer is more evenly distributed with no large differences between median and the 99th and 95th percentiles. It can also be noted from Table 3.2 that the spread among the models is generally larger at the tails of the probability distributions independent of whether there is a bias or not.

3.3 Terrestrial Water Storage

An appropriate model-representation of the seasonal cycle of terrestrial water storage (mainly soil moisture, groundwater, surface water and snow cover) is necessary due to its importance for soil-moisture precipitation feedback (e.g. Betts et al. 1996, Eltahir 1998, Schär et al. 1999), for soil moisture memory effects (e.g. Koster and Suarez 2001, Seneviratne et al. 2005), as well as in relation with the sensitivity of summer climate variability to land-surface processes (e.g. Seneviratne et al. 2002, Schär et al. 2004, Vidale et al. 2005).

The diagnostic data set used here for the analysis and validation of simulated terrestrial water storage (Seneviratne et al. 2004; Hirschi et al. 2005; data download at http://www.iac.ethz.ch/data/water_balance/[1]) was derived with the combined atmospheric and terrestrial water-balance approach using

$$\frac{\P S}{\P t} = -\frac{\P W}{\P t} - \nabla_H \cdot \dot{Q} - R \ . \qquad (1)$$

Here S represents the terrestrial water storage. The atmospheric moisture content W and the horizontal divergence of the vertically integrated atmospheric water vapor flux $\nabla_H \cdot \vec{Q}$ are taken from the ERA-40 reanalysis. For the term R conventional runoff data are used. This derived data set constitutes a useful tool for the validation of large-scale climate and hydrological data (e.g. van den Hurk et al. 2005, Stöckli et al. 2005, and Seneviratne et al. 2005).

[1] The web-page is currently under development and will be available with the publication of Hirschi et al. 2005.

Figure 3.3 shows a comparison of the mean seasonal cycles of the diagnosed terrestrial water storage variations against control runs of the PRUDENCE models in two domains. The first is a combined domain covering Central European river basins (the Rhone, Loire, Seine, Rhine, Po, Weser, Elbe, Odra, Wisla and the northern part of the Danube river basins), the second covers the whole Danube river basin. The results display substantial differences between the models. In Central Europe, most models overestimate the decrease in terrestrial water storage during summer (the drying of the soil) substantially compared to the diagnostic water-balance estimates. In the Danube region, several models underestimate the summer drying by up to 1 mm/d. There are also considerable deficiencies in winter (likely related to the representation of snow). Van den Hurk et al (2005) showed that the soil storage reservoir in an RCM plays an important role in the response of runoff to an A2 emission scenario. A larger storage reservoir makes the RCM runoff less sensitive to changes in precipitation and evaporation, since the effectes of these changes on runoff are buffered by the soil storage. For the temperature climate this is illustrated in Lenderink et al. (2005), Vidale et al., (2005) and Kjellström et al. (2005b).

4. Summary and conclusion

One source of the uncertainty in possible future climate change simulations is related to the model performance. In PRUDENCE, a set of ten regional climate models has been used to simulate current and future climate conditions for Europe. Their results for today's climate have been carefully validated against independent data sets, mainly the CRU data, to be able to judge the quality of model performance. This also shows how the main model systematic biases vary across the different models

and regions.

The analysis of near-surface air temperature and precipitation for the time period 1961 to 1990 shows, in general, a warm bias with respect to the CRU data set in the extreme seasons and a tendency to cold biases in the transition seasons. In winter a typical spread (standard deviation) between the models is 1K. The high inter-annual variability in the observations makes this difference less significant (the CRU mean temperature is only claimed to be accurate to within approximately 1K). The inter-annual variability of the regional models is reduced compared to observations in most areas, particularly in northern and western Europe. This suggests that the driving HadAM3H model is probably too zonal and simulates insufficient amounts of blocking events, which are the main source for the inter-annual variability in this season.

During summer there is generally a better agreement between observed and simulated values of inter-annual variability although there is a relatively clear signal in that most of the modeled temperature variability is larger than suggested by observations, while precipitation variability is closer to observations. The origin of this finding is less easy to interpret. However, the dependency on the formulation of the models surface scheme, particularly during this season offers one possible source for this variability. In summer, the ensemble mean model bias is in general lower than in winter (with the exceptions of MD and EA).

The RCMs reproduce the circulation patterns of the driving GCM well. However, in many regions there are substantial differences between the GCM and RCM surface temperature and precipitation simulations for some RCMs. There is no clear correlation of differences with regions but some

models have region and season independent tendencies to deviate in terms of temperature or precipitation.

A comparison of the HIRHAM experiments at different resolution as well as between the two RCAO experiments shows that changing of resolution has a minor impact on large scale climate features.

The biases in maximum temperatures during summer and minimum temperatures during winter are found to be larger at the extremes than in the mean values. It is found that the RCMs generally underestimate the maximum temperatures during summer in northern Europe while there is an overestimation in eastern Europe. In winter minimum temperatures are overestimated over most of Europe. It is also noted that the spread between the models is generally larger at the tails of the probability distributions than in the median.

A new basin-scale water balance dataset of monthly terrestrial water-storage variations is used for the validation of terrestrial water storage in the control simulations in two regions: a Central European domain combining several smaller river basins and the Danube river basin. The main results of this validation are as follows: during summer, most models overestimate the decrease in terrestrial water storage in the Central European domain, while there tends to be an underestimation of summer drying in the Danube river basin. During winter, some deficiencies are also found in the simulations, corresponding to either over- or underestimation of soil water recharge.

This paper focuses on the validation of the 1961-1990 present-day simulations as input to the assessment of the models' response to climate change. And the primary aim of this paper is to identify how the main model systematic biases vary across the different models. Here mostly qualitative

statements were presented. The determination of quantitative measures is a major focus within the European project ENSEMBLES. Furthermore future work will focus on the following questions: How large are the climate-change signals compared to the biases? Can the differences in climate-change signals between the models be explained based on their different biases? Are the climate change signals affected by systematic biases and how are they affected?

5. References

Anthes, R. A., Hsie, E.-Y., and Kuo, Y.-H.: 1987, 'Description of the Penn State/NCAR Mesoscale Model Version 4 (MM4)', *NCAR Technical Note* **282**, NCAR, Boulder, CO 80307.

Betts, A.K., Ball, J.H., Beljaars, A.C.M., Miller, M.J., and Viterbo, P.A.: 1996, 'The land-surface atmosphere interaction: A review based on observational and global modeling perspectives', *J. Geophys. Res.*, **101**,7209-7225.

Bringfelt, B., Räisänen, J., Gollvik, S., Lindström, G., Graham, L. P., and Ullerstig, A.: 2001, 'The land surface treatment for the Rossby Centre Regional Atmospheric Climate Model version 2 (RCA2)', *Reports Meteorology and Climatology*, **98**, 40pp., *Swedish Meteorological and Hydrological Institute*, Norrköping, Sweden.

Bougeault P.: 1985, 'A simple parameterization of the large-scale effects of cumulus convection', *Mon. Wea. Rev.*, **113**, 2108-2121.

Buonomo E., Jones, R., Huntingford, C., and Hannaford, J.: 2006,'The robustness of high resolution predictions of changes in extreme rainfall for Europe', *Quart. J. R. Meteor. Soc.*, in press.

Castro, M., Fernandez, C. and Gaertner, M.A.: 1993, 'Description of a meso-scale atmospheric numerical model'. In 'Mathematics, Climate and Environment' J.I. Diaz and J.L. Lions (eds.), Masson (ISBN: 2-225-84297-3), 273 pp.

Christensen, J. H., Christensen, O.B., Lopez, P., Van Meijgaard, E., and Botzet,M.: 1996, 'The HIRHAM4 Regional Atmospheric Climate Model', *Scientific Report*, **96-4**, 51 pp., *DMI*, Copenhagen.

Christensen, O. B., Christensen, J.H., Machenhauer, B., and Botzet, M.: 1998, 'Very High-Resolution Regional climate Simulations over Scandinavia - Present Climate', *J. Climate*, **11**, 3204-3229.

Christensen, J.H., Carter, T.R., and Giorgi, F.: 2002, 'PRUDENCE employs new methods to assess European climate change', *EOS*, **83**, 147.

Christensen, J.H., Carter, T.R., and Rummukainen, M.: 2006 'Evaluating the performance and utility of regional climate models: the PRUDENCE project', *Climatic Change*, this issue.

Christensen, J.H., and Christensen, O.B.: 2006, 'A summary of the PRUDENCE model projections of changes in European climate during this century', *Climatic Change*, this issue.

Cubasch U., Waszkewitz, J., Hegerl, G., and Perlwitz, J.: 1995, 'Regional climate changes as simulated in time-slice experiments', *Climate Change*, **31**, 273-304.

Cox, P., Betts, R., Bunton, C., Essery, R., Rowntree, P.R., and Smith, J.: 1999, 'The impact of new land surface physics on the GCM simulation of climate and climate sensitivity', *Climate Dynamics*, **15**, 183-203.

Davies, H.C.: 1976, 'A lateral boundary formulation for multi-level prediction models', *Quart. J. R. Meteor. Soc.*, **102**, 405-418.

Déqué M., Piedelievre, JP.: 1995, 'High resolution climate simulation over Europe', *Climate Dynamics*, **11**, 321-339.

Dickinson, R.E.: 1984, 'Modeling evapotranspiration for the three-dimensional global climate models', in Hansons, JE., and Takahashi, T. (eds.), *Climate Processes and Climate Sensitivity*, *Amer. Geophys. Union*, Washington, DC, pp.58-72.

Dickinson, R.E., Henderson-Sellers, A., and Kennedy, P.J.: 1993, 'Biosphere-Atmosphere Transfer Scheme (BATS) Version 1e as coupled to the NCAR Community Climate Model', *NCAR technical Note*, NCAR-TN-387+STR, NCAR, Boulder, 72 pp.

Döscher, R., Willén, U., Jones, C., Rutgersson, A., Meier, H. E. M., Hansson, U. and Graham, L. P.: 2002, 'The development of the coupled regional ocean-atmosphere model RCAO', Boreal Env. Res., **7**, 183-192.

Douville, H., Chauvin, F. , Royer, J.F., Stephenson, D.B., Tyteca, S., Kergoat, L., Lafont, S., Betts, R.A.: 2000, 'The importance of vegetation feedbacks in doubled-CO2 time-slice experiments', *J. Geophys. Res.*, **105**, 14841-14861.

Ducoudré, N., Kaval, K., Perrier, A., Sechiba: 1993, 'a new set of parameterizations of the hydrologic exchanges at the land-atmosphere interface within the LMD atmospheric general circulation model', *J. Climate*, **6**, 248-273.

Dümenil, L., and Todini, E.: 1992, 'A rainfall-runoff scheme for use in the Hamburg climate model', in O'Kane, J.P. (editor), *Advances in Theoretical Hydrology*, *EGS Series of Hydrological Sciences*, **1**, Elsevier, 129-157.

Edwards, J.M. and Slingo, A.: 1996, 'Studies with a flexible new radiation code. I: Choosing a configuration for a large scale model', *Quart. J. R. Meteor. Soc.*, **122**, 689-719.

Eltahir, E.A.B.: 1998, 'A soil moisture-rainfall feedback mechanism. 1. Theory and observations', *Water Resources Research*, **34**, 765–776.

Garand, L.: 1983, 'Some improvements and complements to the infrared emissivity algorithm including a parameterization of the absorption in the continuum region', *J. Atmos. Sci.*, **40**, 230-244.

Gibelin, A.L., and Déqué, M.: 2003, 'Anthropogenic climate change over the Mediterranean region simulated by a global variable resolution model', *Climate Dynamics*, **20**, 327-339.

Gibson, J.K., Kållberg, P., Uppala, S., Hernandez, A., Nomura,A., and Serrano,E.: 1997, 'Era description', *ECMWF Reanal. Proj. Rep. Ser. 1*, *Eur. Cent. for Medium-Range Weather Forecasting*, Geneva.

Giorgetta, M. and Wild, M., 1995: 'The water vapour continuum and its representation in ECHAM4', *Max Planck Institut für Meteorologie Report*, **162**, 38pp.

Giorgi, F., Marinucci, M.R., Bates, G.T., and DeCanio, G.: 1993, 'Development of a second generation regional climate model (REGCM2). Part II: Cumulus cloud and assimilation of lateral boundary conditions', *Mon. Wea. Rev.*, **121**, 2814-2832.

Giorgi, F., and Mearns, L.O.: 1999, 'Introduction to special section: regional climate modeling revisited', *J. Geophys. Res.*, **104**, 6335- 6352.

Giorgi, F., Huang, Y., Nishizawa, K., and Fu, C.: 1999, 'A seasonal cycle simulation over eastern Asia and its sensitivity to radiative transfer and surface processes', *J. Geophys. Res.*, **104**, 6403-6423.

Giorgi, F., Hewitson, B., Christensen, J.H., Hulme, M., von Storch, H., Whetton, P., Jones, R., Mearns, L., and Fu, C.: 2001, 'Regional Climate Information – Evaluation and Projections', in Houghton, J. et al. (eds.), *Climate Change 2001: The Scientific Basis.*, Intergovernmental Panel on Climate Change, Cambridge University Press.

Gregory, D., and Rowntree, P.R.: 1990, 'A mass-flux convection scheme with representation of cloud ensemble characteristics and stability dependent closure', *Mon. Wea. Rev.*, **118**, 1483-1506.

Gregory, D., and Allen, S.: 1991, 'The effect of convective downdraughts upon NWP and climate simulations', *Ninth conference on numerical weather prediction*, 122-123, Denver, Colorado.

Gregory, D., Kershaw, R., and Inness, P.M.: 1997, 'Parametrization of momentum transport by convection. II: tests in single column and general circulation models', *Quart. J. R. Meteor. Soc.*, **123**, 1153-1183.

Grell, G.A.: 1993, 'Prognostic evaluation of assumptions used by cumulus parameterizations', *Mon. Wea. Rev.*, **121**, 764-787.

Hirschi, M., Seneviratne, S.I., and Schär, C.: 2005, 'Seasonal variations in terrestrial water storage for major mid-latitude river basins', *Journal of Hydrometeorology*, **7 (1),** 39-60..

Houghton, J.T. et al.: 2001, 'Climate Change 2001: The Scientific Basis', Contribution of Working Group I to the Third Assessment Report of the Governmental Panel on Climate Change, Cambridge University Press.

Hsie, E.-Y., Anthes, R. A., Keyser, D.:1984, 'Numerical simulation of frontogenesis in a moist atmosphere', *J. Atmos. Sci*., **41**, 2581-2594.

Hulme, M., Conway, D., Jones, P.D., Barrow, E.M., Jiang, T., and Turney, C.: 1995, 'A 1961-90 climatology for Europe for climate change modelling and impacts applications', *Int. J. Climatol*., **15**, 1333-1363.

Jacob, D.: 2001, 'A note on the simulation of the annual and inter-annual variability of the water budget over the Baltic Sea drainige basin', *Met. Atmos. Phys*., **77**, 61-73

Jacobsen, I. and Heise, E.: 1982, 'A new economic method for the computation of the surface temperature in numerical models', *Beitr. Phys. Atm.*, **55**, 128-141.

Jones, C.G., Willén, U., Ullerstig, A. and Hansson, U.: 2004, 'The Rossby Centre Regional Atmospheric Climate Model Part I: Model Climatology and Performance for the Present Climate over Europe', *Ambio*, **33**:4-5, 199-210.

Jones, R.G., Murphy, J.M., and Noguer, M.: 1995, 'Simulation of climate change over Europe using a nested regional-climate model I: Assessment of control climate, including sensitivity to location of lateral boundaries', *Quart. J. R. Meteor. Soc.*, **121**, 1413-1449.

Kain, J., and Fritsch, J. M.: 1990, 'A one dimensional entraining/detraining plume models and its application to convective parameterization', *J. Atmos. Sci*., **47**, 2784-2802.

Kalnay, E., Kanamitsu, M., Kistler, R., Collins, W., Deaven, D., Gandin, L., Iredell, M., Saha, S., White, G., Woollen, J., Zhu, Y., Chelliah, M., W. Ebisuzaki, W. Higgins, J. Janowiak, K.C. Mo, C. Ropelewski, A. Leetmaa, R. Reynolds, and R. Jenne : 1996, 'The NCEP/NCAR Reanalysis Project', *Bull. Amer. Meteor. Soc.*, **77**, 437-471.

Kessler, E.: 1969, 'On the distribution and continuity of water substance in atmospheric circulation models', *Meteor. Monographs*, **10**, *Americ. Meteor. Soc.*, Boston, MA.

Kiehl, J.T., Hack, J.J., Bonan, G.B., Boville, B.A., Briegleb, B.B., Williamson, D.L., and Rasch, P.J.: 1996, 'Description of the NCAR Community Climate Model (CCM3)', *NCAR technical Note*, NCAR/TN-420+STR, 152 pp.

Kjellström, E., Bärring, L., Jacob, D., Jones, R., Lenderink, G and Schär, C.: 2005, 'Variability in daily maximum and minimum temperatures: recent and future changes over Europe', Submitted to *Climatic Change*.

Klein Tank, A.M.G., Wijngaard, J.B., Können, G.P., Böhm, R., Demarée, G., Gocheva, A., Mileta, M., Pashiardis, S., Hejkrlik, L., Kern-Hansen, C., Heino, R., Bessemoulin, P., Müller-Westermeier, G., Tzanakou, M., Szalai, S., Pálsdóttir, T., Fitzgerlad, D., Rubin, S., Capaldo, M., Maugeri, M., Leitass, A., Bukantis, A., Aberfeld, R., van Engelen, A.F.V., Førland, E., Mietus, M., Coelho, F., Mares, C., Razuvaev, V., Nieplova, E., Cegnar, T., Antonio López, J., Dahlström, B., Moberg, A., Kirchhofer, W., Ceylan, A., Pachaliuk, O., Alexander, L.V., and Petrovic, P.: 2002a, 'Daily dataset of 20th-century surface air temperature and precipitation series for the European Climate Assessment', *Int. J. Climatol*., **22**, 1441-1453.

Klein Tank, A.M.G., Wijngaard, J.B., and van Engelen, A.F.V.: 2002b, 'Climate of Europe. Assessment of observed daily temperature and precipitation records', KNMI, De Bilt, the Netherlands, 36 pp.

Koster, R.D., and Suarez, M.J.: 2001, 'Soil moisture memory in climate models', *J. Hydrometeor*., **2**, 558-570.

Lenderink, G., van den Hurk, B., van Meijgaard, E., van Ulden, A., and Cujipers, H: 2003, 'Simulation of present-day climate in RACMO2: first results and model developments', *KNMI Technical Report*, **252**, 24pp.

Lenderink, G., van Ulden, A., van den Hurk, B. and van Meijngaard, E.: 2006, 'Summertime inter-annual temperature variability in an ensemble of regional model simulations: analysis of the surface energy budget', *Climatic Change*, this issue.

Lin Y.-L., Farley, R.D., and Orville, H.D.: 1983, 'Bulk parameterization of the snow field in a cloud model', *J. Clim. Appl. Meteorol*., **22**, 1065-1095.

Machenhauer, B., Windelband, M., Botzet, M., Christensen, J.H., Déqué, M., Jones, R.G., Ruti, P.M., and Visconti, G.: 1998, 'Validation and analysis of regional present-day climate and climate change simulations over Europe', *Max Planck Intitut für Meteorologie Report*, **275**, *MPI*, Hamburg, Germany.

Meier, H.E.M., Döscher, R., and Faxen, T.: 2003, 'A multiprocessor coupled ice-ocean model for the Baltic Sea. Application to the salt inflow.', *J. Geophys. Res*., **108**, C8:3273.

Morcrette, J-J.: 1990, 'Impact of changes to the radiation transfer parameterizations plus cloud optical properties in the ECMWF model', *Mon. Wea. Rev*., **118**, 847-873.

Morcrette, JJ.: 1989, 'Description of the radiation scheme in the ECMWF model', *ECMWF Technical Memorandum*, **165**, Reading, UK.

Morcrette, J-J.: 1991, 'Radiation and cloud radiative properties in the ECMWF forecasting system', *J Geophys Res*, **96**, 9121-9132.

Nakicenovic, N., Alcamo, J., Davis, G., de Vries, B., Fenhann, J., Gaffin, S., Gregory, K., Grübler, A., Jung, T.Y., Kram, T., La Rovere, E.L., Michaelis, L., Mori, S., Morita, T., Pepper, W., Pitcher, H., Price, L., Raihi, K., Roehrl, A.,

Rogner, H-H., Sankovski, A., Schlesinger, M., Shukla, P., Smith, S., Swart, R., van Rooijen, S., Victor, N., and Dadi, Z.: 2000, 'IPCC Special Report on Emissions Scenarios', Cambridge University Press, Cambridge, United Kingdom and New York, NY, USA.

New M., Hulme M., and Jones P.: 2000, 'Representing twentieth-century space-time climate variability. Part II: Development of 1901-96 monthly grids of terrestrial surface climate', *J. Climate*, **13**, 2217-2238.

New, M., Lister D.,, Hulme, M., and Makin, I.: 2002, 'A high-resolution data set of surface climate over global land areas', *Climate Res.*, **21**, 1-25

Noguer M., Jones R.G., and Murphy, J.M.: 1998, 'Sources of systematic errors in the climatology of a regional climate model over Europe', *Climate Dynamics*, **14**, pp.691-712.

Nordeng, T.E.: 1994, 'Extended versions of the convective parametrization scheme at ECMWF and their impact on the mean and transient activity of the model in the tropics', *Technical Momorandum*, **206**, 41 pp, *European Centre for Medium Range Weather Forecasts*, Reading, UK.

Pal, J.S., Small, E.E., and Eltahir, E.A.B.: 2000, 'Simulation of regional scale water and energy budgets: representation of sub-grid cloud and precipitation processes within RegCM', *J. Geophys. Res.*, **105**, 29579-29594.

Räisänen .J, Hansson, U., Ullerstig, A., Döscher, R., Graham, L.P., Jones, C., Meier, H.E.M., Samuelsson, P., and Willén, U.: 2004, 'European climate in the late twenty-first century: regional simulations with two driving global models and two forcing scenarios', *Climate Dynamics* **22**, 13-31.

Rasch, P. J., and Kristjánsson, J. E.: 1998, 'A comparison of the CCM3 model climate using diagnosed and predicted condensate parameterizations', *J. Climate*, **11**, 1587-1614.

Rayner, N.A., Parker, D.E., Horton, E.B., Folland, C.K., Alexander, L.V., Rowell, D.P., Kent, E.C., and Kaplan, A.: 2003, 'Global analyses of SST, sea ice and night marine air temperature since the late nineteenth century', *J. Geophys. Res.*, **108**, (D14), 4407, doi:10.1029/2002JD002670.

Ricard J.L., and Royer,J.F.: 1993, 'A statistical cloud scheme for use in an AGCM', *Ann. Geophysicae*, **11**, 1095-1115.

Ritter, B., and Geleyn, J.-F.: 1992, 'A comprehensive radiation scheme for numerical weather prediction models with potential applications in climate simulations', *Mon. Wea. Rev.*, **120**, 303-325.

Sass, B. H., Rontu, L, and Räisänen, P.: 1994, 'HIRLAM-2 Radiation Scheme: Documentation and Tests', *HIRLAM Technical Report*, **16**, 43pp., *SMHI*, SE-60176, Norrköping.

Savijärvi, H.: 1990, 'Fast radiation parameterization schemes for mesoscale and short-range forecast models', *J. Appl. Meteor.*, **29**, 437-447.

Schär, C., Lüthi, D., Beyerle, U., and Heise, E.: 1999, 'The Soil-Precipitation Feedback: A Process Study with a Regional Climate Model', *J. Climate*, **12**, 722-741.

Schär, C., Vidale, P.L., Lüthi, D., Frei, C., Häberli, C., Liniger, M.A., and Appenzeller, C.: 2004, 'The role of increasing temperature variability for European summer heat waves', *Nature*, **427**, 332-336.

Seneviratne, S.I., Pal, J.S., Eltahir, E.A.B., and Schär, C.: 2002, 'Summer dryness in a warmer climate: A process study with a regional climate model', *Climate Dynamics*, **20**, 69-85.

Seneviratne, S.I., Viterbo, P., Lüthi, D., and Schär, C.: 2004, 'Inferring changes in terrestrial water storage using ERA-40 reanalysis data: The Mississippi river basin', *J.Climate*, **17**, 2039-2057.

Seneviratne, S.I., Koster, R.D., Guo, Z., Dirmeyer, P.A., Kowalczyk, E., Lawrence, D., Liu, P., Lu, C-H., Mocko, D., Oleson, K.W., and Verseghy, D.: 2005, 'Soil moisture memory in AGCM simulations: Analysis of Global Land-Atmosphere Coupling Experiment (GLACE) data', submitted to *J. Hydrometeorology*.

Simmons, A. J., and J. K. Gibson: 2000, 'The ERA-40 Project Plan', *ERA-40 Project Report Series*, **1**, 63pp, *ECMWF*, Shinfield Park, Reading, UK.

Smith, R. N. B.: 1990, 'A scheme for predicting layer clouds and their water content in a general circulation model', *Quart. J. R. Meteor. Soc.*, **116**, 435-460.

Stephens, G. L.: 1978, 'Radiation profiles in extended water clouds. II: Parameterizaton schemes', *J. Atmos. Sci.*, **35**, 2123-2132.

Steppeler, J., Doms, G., Schaettler, U., Bitzer, H.W., Gassmann, A., Damrath, U., and Gregoric, G.: 2003, 'Meso-gamma scale forecasts using the nonhydrostatic model LM', *Met. Atmos. Phys.*, **82**, 75-96.

Stöckli, R., Vidale, P.L., Boone, A., Hirschi, M., and Schär, C.: 2005, 'Sensitivity of the diurnal and seasonal course of modeled runoff to three different land surface model soil moisture parameterizations', submitted to *J. Hydrometeorology*.

Sundquist, H.: 1978, 'A parameterization scheme for non-convective condensation including precipitation including prediction of cloud water content', *Quart. J. R. Meteor. Soc.*, **104**, 677-690.

Tiedtke, M.: 1989, 'A comprehensive mass flux scheme for cumulus parameterization in large-scale models', *Mon. Wea. Rev.*, **117**, 1779-180.

Van den Hurk, B., Hirschi, M., Schär, C., Lenderink, G., van Meijgaard, E., van Ulden, A., Rockel, B., Hagemann, S., Graham, P., Kjellström, E., and Jones, R.: 2005, 'Soil control on runoff response to climate change in regional climate model simulations', *J. Climate*, **18**, 3536-3551.

Van Ulden, A., Lenderink, G., Van den Hurk, B., and Van Meijgaard, E.: 2005, 'Circulation Statistics and Climate Change in Central Europe: PRUDENCE Simulations and Observations', *Climatic Change*, this issue.

Vidale, P.L., Lüthi, D., Frei, C., Seneviratne, S.I., and Schär, C.: 2003, 'Predictability and uncertainty in a regional climate model', *J. Geophys. Res*., **108,** (D18), 4586, doi:10.1029/2002JD002810.

Vidale, P.L., Lüthi, D., Wegmann, R., and Schär, C.: 2005, 'European climate variability in a heterogeneous multi-model ensemble', *Climatic Change*, this issue.

von Storch, H, Langenberg, H., and Feser, F.: 2000, 'A spectral nudging technique for spectral downscaling purposes', *Mon. Wea. Rev*., **128**, 3664-3673.

Wilby, R.L., Wigley, T.M.L., Conway, D., Jones, P.D., Hewitson, B.C., Main, J., and Wilks, D.S.: 1998, 'Statistical downscaling of General Circulation Model Output: A Comparison of Methods', *Water Resources Research*, **34**, 2995-3008.

Acknowledgements

This research was supported by the Fifth Framework Programme of the European Union (project PRUDENCE, contract EVK2-2000-00132), by the Swiss Ministry for Education and Research (BBW contract 01.0305-1), and by the Swiss National Science Foundation (NCCR Climate). We also like to thank the reviewers for their valuable comments, which helped to improve the final version of the paper.

Figure captions:

Figure. 3.1.1: Mean sea level pressure climatologies. Left column: ERA40, right column: HadAM3H. Upper row: DJF, lower row: JJA. Units in hPa.

Figure. 3.1.2a: Mean sea level pressure climatologies for JJA (Left) and DJF (right) Upper row: GCM, lower row: RCM ensemble. Units in hPa.

Figure. 3.1.2b: Ensemble mean deviation from driving HadAM3H in MSLP based on 10 RCMs (colour) and inter model standard deviation (black contours), levels shown 0.25, 0.5, and 1.0 hPa.

Fig. 3.1.3: A schematic overview of seasonal biases of the PRUDENCE regional models. In each panel, rows are the analysis areas, columns correspond to models. Rows of panels signify the four seasons, the left column of panels are temperature biases (left color bar, degrees C), whereas the right column of panels signifies precipitation (right color bar, relative change). The label HIRHAM No. indicates the simulations done at met.no, as opposed to the HIRHAM simulations done at the DMI. Areas not covered by a particular model are indicated by black squares.

Figure 3.3: Comparison of estimated variations in terrestrial water storage against PRUDENCE model runs for (a) the mean of several Central European river basins (1972-1990, period restricted because of missing runoff data) and (b) the Danube river basin (1961-1990).

Tables

Table 2.1: Summary of grid configurations and parameterizations for the models used in the present study.

Table 3.1.3a: Temperature Bias DJF with respect to the CRU climatology for each of the 8 regions. For some sub-regions fewer models enter the ensemble mean, due to limited coverage by some models. The last entry provides the corresponding CRU mean value. For each sub-region the mean bias (left columns) and the inter-annual standard deviation (right columns) is presented. For the ensemble mean the inter-model standard deviation of the 30-year biases is shown instead.

Table 3.1.3b: Temperature Bias JJA with respect to the CRU climatology for each of the 8 regions. For some sub-regions fewer models enter the ensemble mean, due to limited coverage by some models. The last entry provides the corresponding CRU mean value. For each sub-region the mean bias (left columns) and the inter-annual standard deviation (right columns) is presented. For the ensemble mean the inter-model standard deviation of the 30-year biases is shown instead.

Table 3.1.4a: Precipitation Bias DJF with respect to the CRU climatology for each of the 8 regions. For some sub-regions fewer models enter the ensemble mean, due to limited coverage by some models. The last entry provides the corresponding CRU mean value. For each sub-region the mean bias (left columns) and the inter-annual standard deviation (right columns) is presented. For the ensemble mean the inter-model standard deviation of the 30-year biases is shown instead.

Table 3.1.4b: Precipitation Bias JJA with respect to the CRU climatology for each of the 8 regions. For some sub-regions fewer models enter the ensemble mean, due to limited coverage by some models. The last entry provides the corresponding CRU mean value. For each sub-region the mean bias (left columns) and the inter-annual standard deviation (right columns) is presented. For the ensemble mean the inter-model standard deviation of the 30-year biases is shown instead.

Table 3.2 Bias in T_{2min} and T_{2max} in the 8 European regions defined in Figure 3.1. The bias is given as the median among the ten RCMs and the range is defined as the difference between the two models giving the most differing biases.

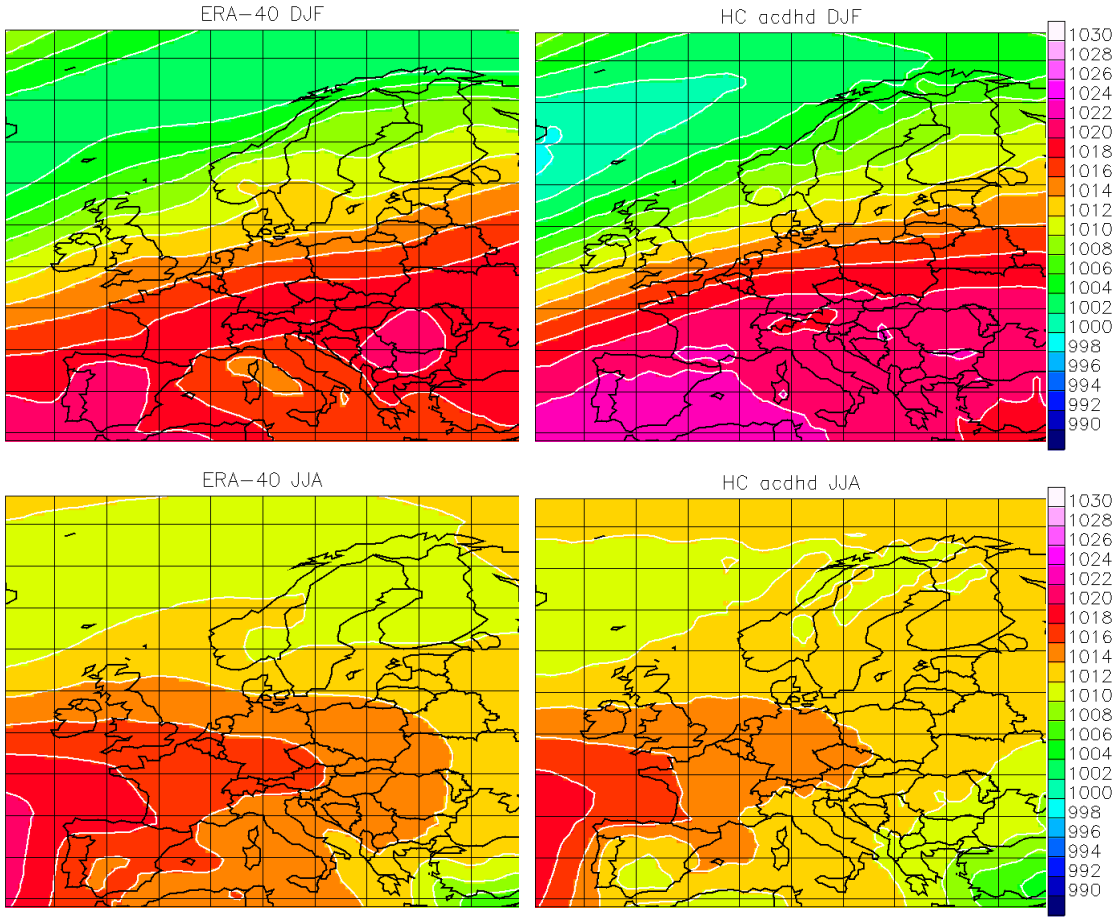

Figure. 3.1.1: Mean sea level pressure climatologies. Left column: ERA40, right column: HadAM3H. Upper row: DJF, lower row: JJA. Units in hPa.

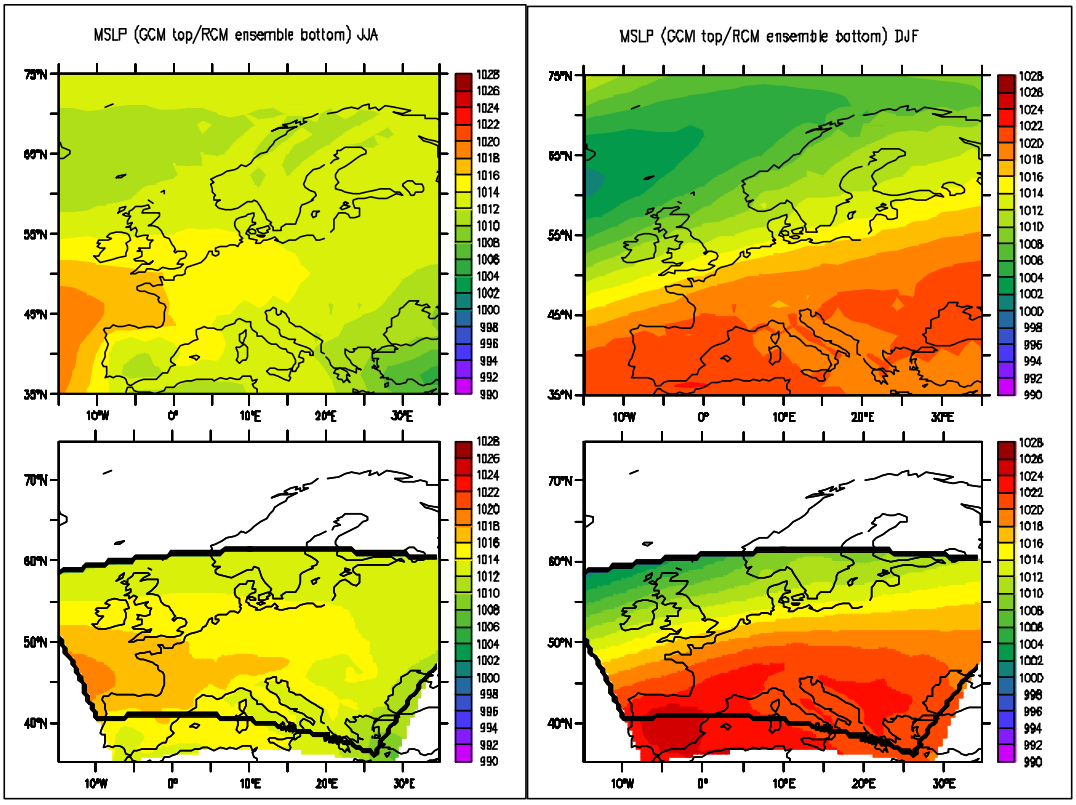

Figure. 3.1.2a: Mean sea level pressure climatologies for JJA (Left) and DJF (right) Upper row: GCM, lower row: RCM ensemble. Units in hPa.

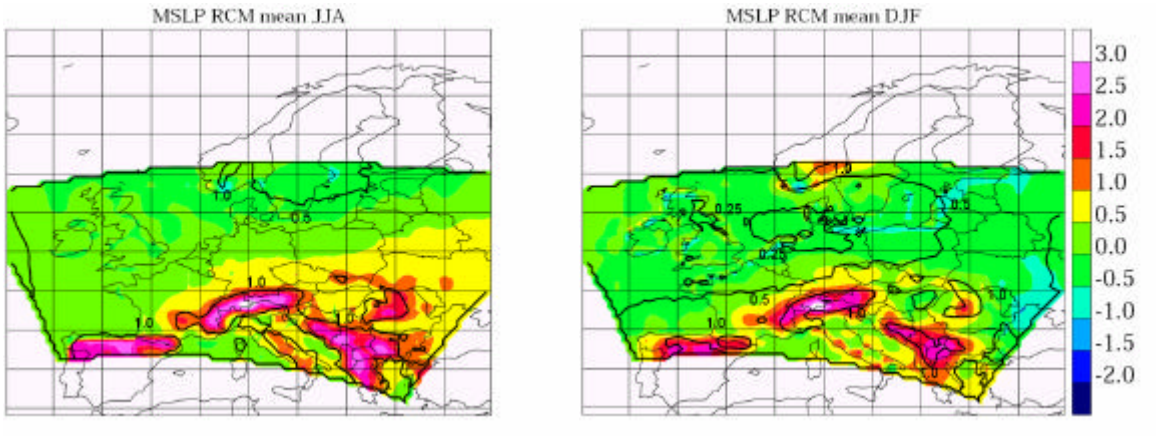

Figure. 3.1.2b: Ensemble mean deviation from driving HadAM3H in MSLP based on 10 RCMs (colour) and inter model standard deviation (black contours), levels shown 0.25, 0.5, and 1.0 hPa.

Fig. 3.1.3: A schematic overview of seasonal biases of the PRUDENCE regional models. In each panel, rows are the analysis areas, columns correspond to models. Rows of panels signify the four seasons, the left column of panels are temperature biases (left color bar, degrees C), whereas the right column of panels signifies precipitation (right color bar, relative change). The label HIRHAM No. indicates the simulations done at the Norwegian Meteorological Office, as opposed to the HIRHAM simulations done at the Danish Meteorological Institute. Areas not covered by a particular model are indicated by black squares.

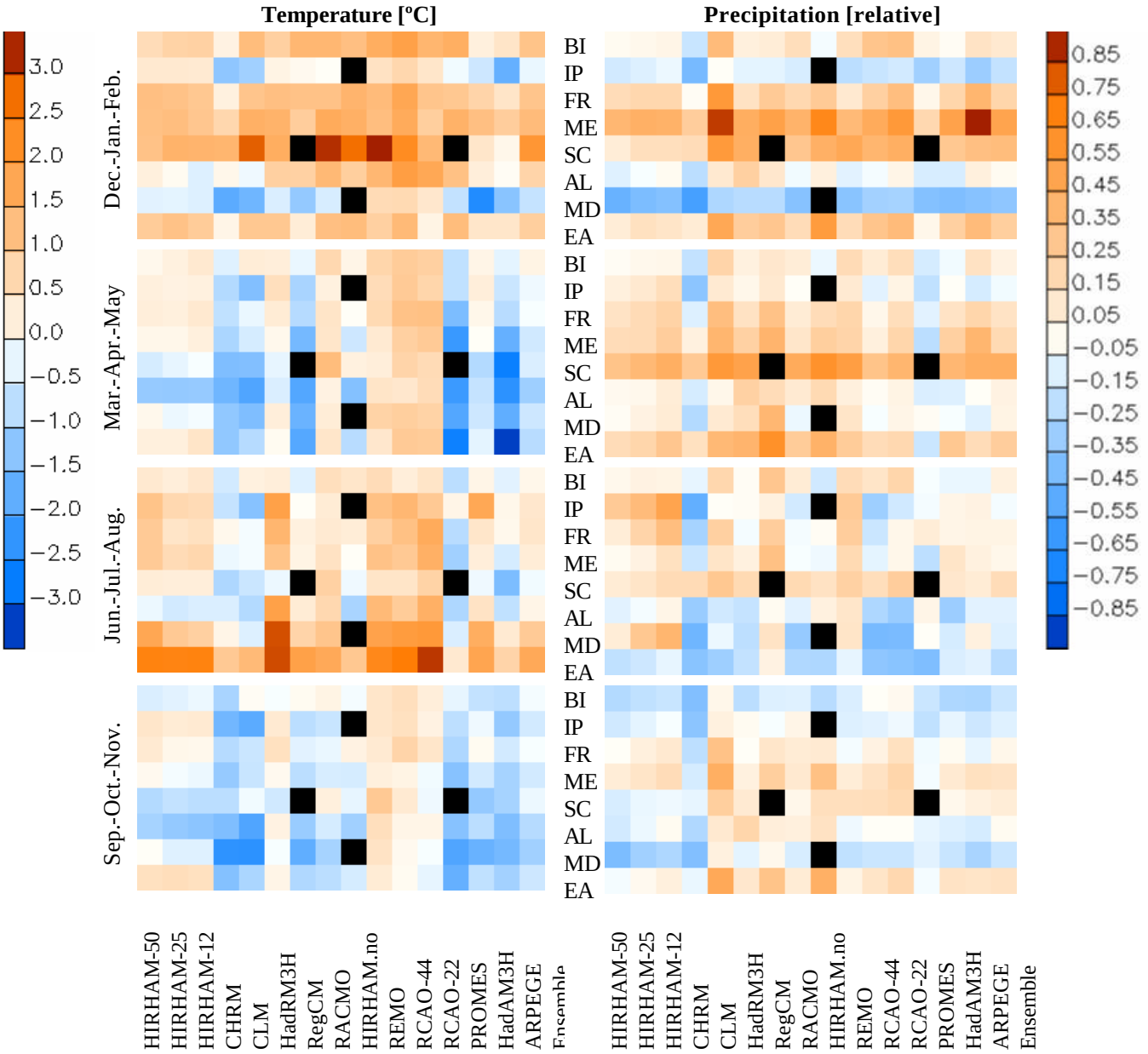

Figure 3.3: Comparison of estimated variations in terrestrial water storage against PRUDENCE model runs for (a) the mean of several Central European river basins (1972-1990, period restricted because of missing runoff data) and (b) the Danube river basin (1961-1990).

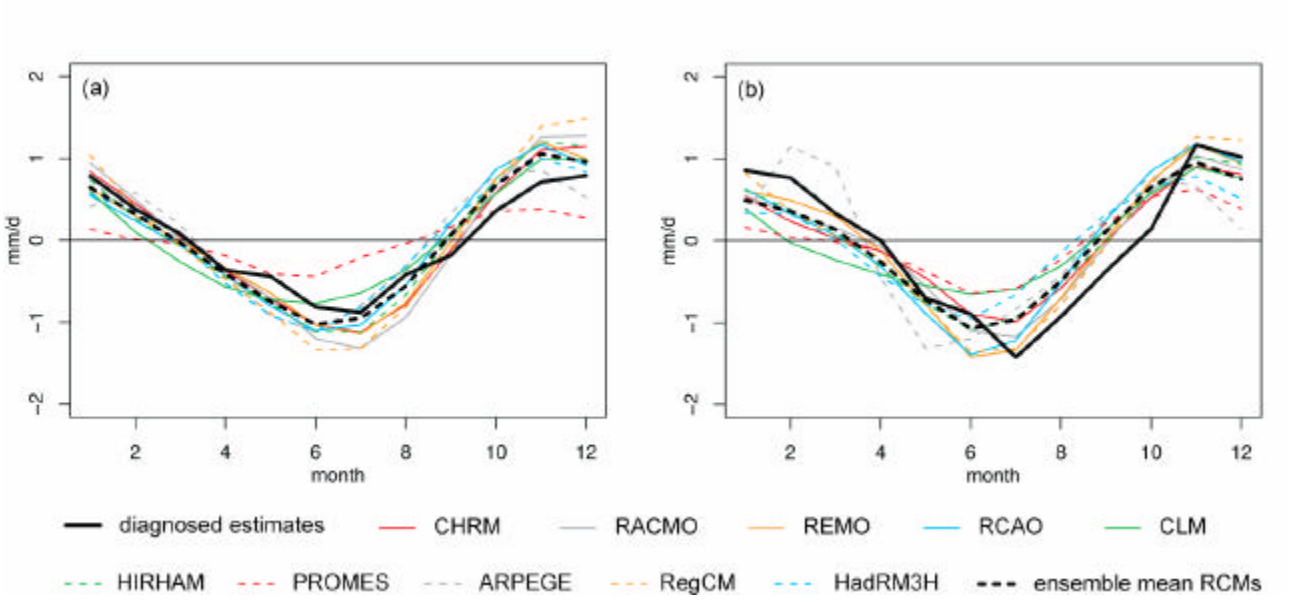

Table 2.1: Summary of grid configurations and parameterizations for the models used in the present study.

	HIRHAM	**ARPEGE**	**CHRM**	**HadRM3H**	**REMO**
Grid resolution	0.44° (50 km)	50-70 km (over Europe)	0.5° (55 km)	0.44° (50 km)	0.5° (55 km)
Grid (lat*lon)	110 x 104	Global, stretched 240 x 120	81 x 91	90 x 95	97 x 109
South pole/rotation	27°E, 37°S	0°E, 90°S	10°E, 32.5°S	10°E, 38°S	10°E, 32.5°S
Vertical levels	19	31	20	19	19
Lateral boundary	Davies, 1976	-	Davies, 1976	-	Davies, 1976
Number of points	10	-	8	4	8
Convection	mass flux Tiedtke, 1989 Nordeng, 1994	mass flux Bougeault, 1985	mass flux Tiedtke 1989	mass flux Gregory & Rowntree, 1990 Gregory & Allen, 1991	mass flux Tiedtke, 1989 Nordeng, 1994 for CAPE closure
Microphysics	Sundqvist, 1978	Ricard & Royer, 1993	Kessler 1969 Lin et al. 1983	Smith, 1990 Jones et al., 1995	Sundqvist, 1978
Radiation	Morcrette, 1991 Giorgetta & Wild, 1995	Morcrette, 1990	Ritter & Geleyn 1992	Edwards & Slingo, 1996	Morcrette, 1989 Giorgetta & Wild, 1995
Land surface	Dümenil & Todini, 1992	ISBA scheme, Douville et al. 2000	Dickinson 1984 Jacobsen & Heise 1982	Cox et al., 1999	Dümenil & Todini, 1992
soil thermal layers	5	4	4	4	5
soil moisture layers	1	2	3	4	1

	RACMO	**RegCM**	**PROMES**	**CLM**	**RCAO**	**HadAM3H**
Grid resolution	0.44° (50 km)	50-70 km , lam. conformal	50 km, lam. conformal	0.5° (55 km)	0.44° (50 km)	1.875° x 1.25°
Grid (lat*lon)	114 x 110	119 x 98	112 x 96	101 x 107	106 x 102	Global, 81 x 91
South pole	23°E, 28°S	-	-	10°E, 32.5°S	25°E, 32°S	-
Vertical levels	31	16	28	20	24 - 60	19
Lateral boundary	Davies, 1976	Giorgi et al. 1993	Davies, 1976	Davies, 1976 von Storch et al, 2000	Davies, 1976	-
Number of points	8 (16 for u,v)	11	10	8	8	-
Convection	mass flux Tiedtke, 1989	mass flux Grell 1993	mass flux, Kain & Fritsch, 1990	mass flux Tiedtke, 1989	mass flux, Kain & Fritsch, 1990	Gregory & Rowntree, 1990 Gregory et al, 1997
Microphysics	-	Pal et al. (2000)	Hsie et al., 1984	Kessler, 1969 Lin et al., 1983	Rasch and Kristjansson, 1998	-
Radiation	Morcrette, 1991	Kiehl et al. 1996, Giorgi et al., 1999	Anthes et al., 1987 Stephens, 1978 Garand, 1983	Ritter & Geleyn, 1992	Savijarvi, 1990 Sass et. al., 1994	Edwards & Slingo, 1996
Land surface	-	Dickinson et al. (1993)	Ducoudre et al., 1993	-	Bringfelt et al., 2001	Cox et al., 1999
soil thermal layers	4	Force-restore	7	9 (at all)	2	-
soil moisture layers	4	3	2		2	-

Table 3.1.3a: Temperature Bias (°C) DJF with respect to the CRU climatology for each of the 8 regions. For some sub-regions fewer models enter the ensemble mean, due to limited coverage by some models. The last entry provides the corresponding CRU mean value. For each sub-region the mean bias (left columns) and the inter-annual standard deviation (right columns) is presented. For the ensemble mean the inter-model standard deviation of the 30-year biases is shown instead.

	BI		IP		FR		ME		SC		AL		MD		EA	
	Bias	I.an	Bias	I.an	Bias	I.an	Bias	I.an	Bias	I.an	Bias	I.an	Bias	I.an	Bias	I. an
HIRHAM	0,70	0,97	0,44	0,79	1,32	1,13	1,28	1,69	1,27	1,76	0,29	1,28	-0,27	1,01	1,05	2,09
HIRHAM25	0,91	0,88	0,43	0,74	1,26	1,04	1,35	1,56	1,59	1,69	0,06	1,26	-0,23	0,93	1,27	1,84
HIRHAM12	0,93	0,94	0,41	0,76	1,14	1,20	1,17	1,63	1,56	1,58	-0,34	1,35	-0,32	0,98	1,04	1,81
CHRM	0,23	0,91	-1,19	0,63	0,27	0,94	0,82	1,19	1,53	1,56	0,15	0,90	-1,78	0,84	0,17	1,66
CLM	1,37	0,78	-1,01	0,72	1,19	0,98	1,63	1,24	2,98	1,25	-0,13	1,03	-1,56	0,86	1,15	1,57
HadRM3H	0,98	0,99	0,20	0,80	1,31	1,18	1,57	1,49	1,71	1,66	0,96	1,17	-0,34	0,89	1,15	1,69
RegCM	1,50	0,85	0,07	0,71	1,27	1,01	1,03	1,27	-	-	0,92	1,11	-1,14	0,86	0,36	1,40
RACMO	1,48	0,84	-	0,68	1,25	1,00	1,76	1,31	3,34	1,45	1,47	1,04	-0,37	0,85	1,33	1,51
HIRHAM.no	1,31	0,89	-	-	1,55	1,01	1,63	1,38	2,88	1,75	0,99	1,23	-	-	1,36	1,62
REMO	1,70	0,82	0,57	0,73	1,41	1,11	1,34	1,47	3,46	1,30	1,49	1,10	0,73	0,81	0,97	1,55
RCAO	1,95	0,72	0,82	0,68	1,84	0,96	1,76	1,38	2,39	1,69	2,01	1,14	0,76	0,87	1,44	1,70
RCAO22	1,54	0,80	0,48	0,71	1,19	1,03	1,01	1,57	1,46	1,71	1,8	1,15	0,48	0,89	0,20	1,96
PROMES	1,67	0,86	-0,08	0,77	1,14	1,13	1,63	1,46	-	-	1,3	1,19	-0,62	0,95	1,38	1,61
HadAM3H	0,28	1,07	-0,49	0,83	0,87	1,15	1,31	1,52	0,5	1,81	0,33	1,28	-2,44	1,17	0,49	1,85
ARPEGE	0,52	0,81	-1,68	0,75	0,53	0,91	1,03	1,13	0,13	1,87	0,04	0,90	-1,26	0,82	0,49	1,64
ENS	1,22	0,54	-0,19	0,83	1,19	0,44	1,41	0,33	2,19	1,11	0,86	0,69	-0,59	0,87	0,99	0,45
CRU	3,56	1,13	6,40	0,85	4,10	1,30	0,75	1,74	-8,69	2,55	-1,11	1,22	4,57	0,79	-2,39	1,91

Table 3.1.3b: As for Table 3.1.3a but for JJA

	BI		IP		FR		ME		SC		AL		MD		EA	
	Bias	I.an	Bias	I.an	Bias	I.an	Bias	I.an	Bias	I.an	Bias	I.an	Bias	I.an	Bias	I.an
HIRHAM	0.43	0.72	1.24	0.84	1.09	1.12	1.08	1.06	0.36	0.78	-0.16	1.01	1.86	1.01	2.60	1.19
HIRHAM25	0.32	0.60	0.78	0.81	0.52	0.94	0.74	0.93	0.31	0.68	-0.43	0.88	1.10	0.97	2.58	1.21
HIRHAM12	0.46	0.56	0.74	0.78	0.61	0.89	0.82	0.87	0.32	0.71	-0.36	0.81	0.95	0.92	2.59	1.04
CHRM	-0.43	0.55	-0.58	0.82	0.12	0.98	-0.13	0.73	-0.84	0.69	-0.34	0.91	0.18	0.87	1.10	0.72
CLM	0.26	0.61	-1.28	0.76	-0.07	0.95	-0.06	0.82	-0.52	0.75	-0.80	0.87	-0.33	0.70	1.44	1.02
HadRM3H	0.33	0.70	1.97	0.97	1.53	1.49	1.23	1.38	-0.13	0.76	1.95	1.45	3.12	1.38	3.12	1.40
RegCM	-0.29	0.67	-0.01	0.95	0.25	1.36	0.21	1.08	-	-	0.37	1.27	0.87	1.20	1.97	1.17
RACMO	0.65	0.50	0.39	0.82	0.41	0.76	0.60	0.59	0.93	0.74	0.80	0.74	1.19	0.81	1.79	0.70
HIRHAM.no	0.50	0.77	-	-	0.36	0.98	0.00	1.04	-0.12	1.01	-0.90	0.83	-	-	1.14	0.88
REMO	0.70	0.51	1.30	0.83	0.96	0.87	1.25	0.84	0.53	0.81	1.44	0.91	1.93	0.96	2.50	1.19
RCAO	0.32	0.55	1.49	0.93	1.30	1.20	1.11	0.96	0.53	0.71	1.06	1.06	2.07	1.06	2.72	0.97
RCAO22	0.54	0.67	1.12	0.88	1.76	1.21	1.65	1.16	0.91	0.79	1.63	1.28	2.14	1.05	3.27	1.13
PROMES	-0.71	0.70	0.17	1.08	-0.72	1.37	-0.98	1.22	-	-	-0.84	1.25	-0.35	0.93	0.44	1.25
HadAM3H	0.17	0.57	1.83	1.08	0.51	1.06	0.33	0.75	-0.12	0.78	0.55	0.92	1.69	1.22	1.88	0.96
ARPEGE	-0.28	0.46	0.14	1.12	0.11	1.20	-0.4	0.69	-1.41	0.67	-0.64	1.08	0.41	1.05	0.89	0.79
ENS	0.14	0.48	0.48	1.01	0.48	0.67	0.36	0.75	-0.07	0.75	0.18	1.01	1.09	1.15	1.79	0.87
CRU	13.82	0.73	20.50	0.69	17.57	0.87	16.66	0.71	12.96	0.82	15.45	0.63	20.65	0.54	17.79	0.63

Table 3.1.4a: As for Table 3.1.3a but for precipitation (mm/day)

	BI		IP		FR		ME		SC		AL		MD		EA	
	Bias	I.an.	Bias	I.an.	Bias	I.an	Bias	I.an	Bias	I.an.	Bias	I.an.	Bias	I.an.	Bias	I.an.
HIRHAM	0,06	0,63	-0,32	1,01	0,45	0,74	0,70	0,67	0,17	0,42	-0,25	0,82	-1,37	0,65	0,13	0,26
HIRHAM25	0,11	0,63	-0,22	1,05	0,52	0,72	0,76	0,69	0,30	0,44	-0,01	0,88	-1,17	0,70	0,22	0,30
HIRHAM12	0,16	0,64	-0,10	1,12	0,53	0,74	0,76	0,71	0,30	0,44	0,05	0,97	-1,11	0,73	0,19	0,29
CHRM	-0,51	0,57	-1,05	0,85	0,01	0,68	0,47	0,60	0,33	0,37	-0,62	0,85	-1,69	0,60	0,14	0,25
CLM	1,30	0,92	0,01	1,13	1,36	1,00	1,51	0,94	1,00	0,46	0,38	1,01	-0,71	0,76	0,66	0,34
HadRM3H	0,27	0,73	-0,17	1,02	0,38	0,76	0,79	0,73	0,78	0,44	0,85	1,11	-0,60	0,94	0,37	0,30
RegCM	0,32	0,74	-0,17	1,02	0,70	0,81	0,91	0,71	-	-	0,41	0,90	-0,62	0,87	0,42	0,31
RACMO	0,63	0,73	-0,26	0,99	0,51	0,78	0,73	0,66	0,55	0,42	-0,07	0,98	-1,07	0,77	0,25	0,28
HIRHAM.no	-0,07	0,57	-	-	0,69	0,74	1,16	0,72	0,77	0,43	0,27	0,95	-	-	0,74	0,29
REMO	0,59	0,81	-0,49	0,98	0,29	0,74	0,67	0,69	0,85	0,42	-0,24	0,89	-1,05	0,82	0,25	0,29
RCAO	1,12	0,81	-0,40	0,92	0,61	0,79	0,82	0,64	0,72	0,49	-0,05	1,01	-0,81	0,81	0,44	0,30
RCAO22	1,19	0,87	-0,31	1,00	0,85	0,82	1,00	0,72	0,79	0,5	0,16	1,01	-0,79	0,82	0,51	0,31
PROMES	0,20	0,72	-0,71	0,89	0,09	0,65	0,36	0,58	-	-	-0,33	0,93	-1,11	0,81	0,05	0,25
HadAM3H	0,03	0,65	-0,35	0,99	0,54	0,80	0,90	0,73	0,54	0,40	-0,34	0,83	-1,14	0,66	0,34	0,29
ARPEGE	0,51	0,64	-0,75	0,58	0,97	0,82	1,61	0,54	0,62	0,35	0,25	0,79	-1,08	0,45	0,50	0,27
ENS	0,40	0,52	-0,43	0,32	0,55	0,39	0,89	0,39	0,64	0,26	0,05	0,42	-1,01	0,34	0,36	0,22
CRU	3,45	0,78	2,66	0,97	2,38	0,62	1,74	0,44	1,76	0,40	3,25	0,71	3,12	0,73	1,34	0,30

Table 3.1.4b: As for Table 3.1.4a but for JJA

	BI		IP		FR		ME		SC		AL		MD		EA	
	Bias	I.an.	Bias	I.an.	Bias	I.an	Bias	I.an	Bias	I.an.	Bias	I.an.	Bias	I.an.	Bias	I.an.
HIRHAM	0,09	0,51	0,31	0,31	0,17	0,39	0,04	0,46	0,24	0,37	-0,28	0,47	0,14	0,31	-0,44	0,47
HIRHAM25	0,15	0,49	0,41	0,28	0,44	0,36	0,14	0,41	0,33	0,35	-0,07	0,55	0,45	0,41	-0,34	0,52
HIRHAM12	0,14	0,46	0,56	0,32	0,66	0,39	0,40	0,53	0,47	0,27	0,20	0,53	0,61	0,44	-0,13	0,53
CHRM	-0,14	0,57	-0,50	0,27	-0,47	0,40	-0,33	0,48	0,46	0,39	-1,15	0,64	-0,62	0,44	-0,86	0,45
CLM	0,55	0,62	0	0,31	0,47	0,45	0,33	0,52	0,73	0,31	-0,51	0,66	-0,06	0,55	-0,70	0,44
HadRM3H	0,02	0,57	0,01	0,34	-0,02	0,50	0,17	0,65	0,49	0,34	-0,63	0,95	-0,27	0,50	-0,43	0,61
RegCM	0,79	0,67	0,07	0,35	0,51	0,58	0,82	0,64	-	-	0,07	0,72	0,22	0,68	0,16	0,72
RACMO	0,26	0,52	-0,13	0,31	-0,03	0,35	-0,01	0,43	0,49	0,37	-0,28	0,68	-0,44	0,44	-0,56	0,42
HIRHAM.no	-0,32	0,46	-	-	0,01	0,46	-0,08	0,36	0,38	0,44	0,28	0,72	-	-	-0,57	0,40
REMO	0,47	0,62	0,32	0,34	0,50	0,53	0,48	0,55	0,59	0,36	0,53	0,64	0,22	0,58	-0,14	0,64
RCAO	0,35	0,58	-0,30	0,27	-0,26	0,42	-0,15	0,49	0,43	0,32	-0,91	0,76	-0,58	0,43	-0,83	0,47
RCAO22	0,57	0,68	-0,13	0,33	0,07	0,44	0,09	0,59	0,66	0,36	-1,15	0,70	-0,58	0,39	-0,87	0,55
PROMES	-0,01	0,46	-0,02	0,31	0,17	0,43	-0,43	0,44	-	-	0,20	0,71	0	0,50	-0,95	0,42
HadAM3H	-0,11	0,47	0,06	0,35	0,08	0,45	0,33	0,48	0,29	0,27	-1,13	0,49	-0,16	0,36	-0,24	0,43
ARPEGE	-0,12	0,42	0,07	0,33	0,10	0,51	0,16	0,43	0,23	0,27	-0,28	0,71	0,10	0,45	-0,18	0,38
ENS	0,18	0,34	-0,02	0,25	0,11	0,31	0,09	0,36	0,45	0,16	-0,27	0,51	-0,13	0,32	-0,50	0,34
CRU	2,50	0,55	1,09	0,33	1,84	0,46	2,35	0,45	2,38	0,35	3,99	0,74	1,49	0,42	2,56	0,36

Table 3.2 Bias in T_{2min} and T_{2max} in the 8 European regions defined in Figure 3.1. The bias is given as the median among the ten RCMs and the range is defined as the difference between the two models giving the most differing biases.

Variable		Percentile	BI	IP	FR	ME	SC	Al	MD	EA
DJF										
	T_{2min} median	1	5.9	2.6	5.3	3.0	5.3	0.5	1.0	-0.3
		5	5.3	2.2	3.4	3.4	5.1	0.5	0.6	-0.7
		50	2.9	1.0	2.6	1.5	3.1	1.5	0.3	-0.1
	T_{2min} range	1	6.6	5.9	5.7	6.4	9.9	11.3	9.7	9.9
		5	5.9	5.1	6.8	4.2	5.1	8.2	8.8	5.0
		50	3.0	3.7	2.9	1.9	3.6	5.2	5.0	4.0
JJA										
	T_{2max} median	50	-1.2	1.4	0.2	-1.4	-2.6	-1.3	0.7	0.6
		95	-2.2	1.1	0.7	-0.2	-3.3	0.2	0.9	2.6
		99	-2.8	0.6	0.8	0.5	-3.3	0.8	0.2	3.0
	T_{2max} range	50	2.9	3.2	5.8	5.2	1.9	5.6	5.6	5.3
		95	3.7	6.5	6.4	5.4	4.0	9.0	9.0	6.5
		99	6.8	7.9	8.2	7.5	5.2	10.4	10.4	7.6